

Synthesis of Colloidal Uranium–Dioxide Nanocrystals

Huimeng Wu, Yongan Yang, and Y. Charles Cao*

Department of Chemistry, University of Florida, Gainesville, Florida 32611

Received November 6, 2006; E-mail: cao@chem.ufl.edu

In the past half-century, uranium–oxides have become important materials for technological applications. Enriched uranium–dioxide is the major component of the fuel materials for nuclear reactors.¹ Depleted uranium–oxides can be used for radiation shielding,¹ and they are also highly efficient and stable catalysts for the destruction of chlorine-containing organic pollutants at moderate temperatures.² In addition, uranium–dioxide is a material with a high Seebeck coefficient,³ which is potentially important to thermopower applications.

Because nanomaterials can exhibit solution processability as well as size-dependent physical and chemical properties,⁴ the ability to synthesize high-quality, colloidal uranium–oxide nanocrystals would create a new opportunity to facilitate uranium–oxide-based applications. However, less is known about the synthesis of colloidal uranium–oxide nanocrystals at high quality.⁵ Herein, we report an organic-phase synthesis method for producing nearly monodispersed UO₂ nanocrystals as well as the mechanisms for controlling the nanocrystal formation.

The uranium–oxide nanocrystals were synthesized by thermal decomposition of uranyl acetylacetonate (UAA) in a mixture solution of oleic acid (OA), oleylamine (OAm), and octadecene (ODE). In a typical synthesis, UAA (0.4 mmol) was dissolved in a solution of OA (1.0 g) and ODE (1.0 g) at 150 °C.⁶ After the solution was cooled to room temperature, OAm (1.0 g) was added, and then the resulting mixture was degassed under vacuum (~20 mTorr) at 100 °C for 10 min. Under Ar flow, the reaction solution was heated to 295 °C at a rate of 35 °C/min and aged at the same temperature for 5 min, and then the solution was cooled to room temperature. The nanocrystals were precipitated from the reaction solution by adding a mixture of hexane and acetone (1:4), and the black nanocrystal precipitate can be easily re-dispersed in nonpolar organic solvents, such as hexane.

Transmission electron microscopy (TEM) shows that the uranium–oxide nanocrystals are nearly monodispersed, spherical particles with a diameter of 5.4 nm and a standard deviation of 2.6% (Figure 1a). X-ray powder diffraction (XRD) shows that the nanocrystals consist of uranium–dioxide (Figure 1b). The XRD pattern of the nanocrystal sample exhibits the highly crystalline peaks that can be indexed to nearly all the Bragg reflections corresponding to the standard face-centered cubic (fcc) structure of UO₂ (*Fm*3*m*, *a* = 0.5468 nm). These Bragg reflections are quite distinguishable from those of the typical crystal structures of other uranium–oxides such as U₃O₈ and UO₃.⁶ Moreover, this structural assignment is consistent with high-resolution TEM (HRTEM) observation (inset of Figure 1b). A HRTEM image of the nanocrystal sample shows the characteristic cross-fringe pattern of the fcc crystal structure viewed along the [011] zone axis. The ordered distance of 0.32 nm shown in the high-resolution image—corresponding to the lattice spacing of the (111) faces in the fcc UO₂—is in good agreement with the result from the XRD measurement.

The formation of uranium–dioxide indicates that reduction of U(VI) to U(IV) is included in the nanocrystal synthesis. The reaction yield of the typical nanocrystal synthesis is about 78%. In addition,

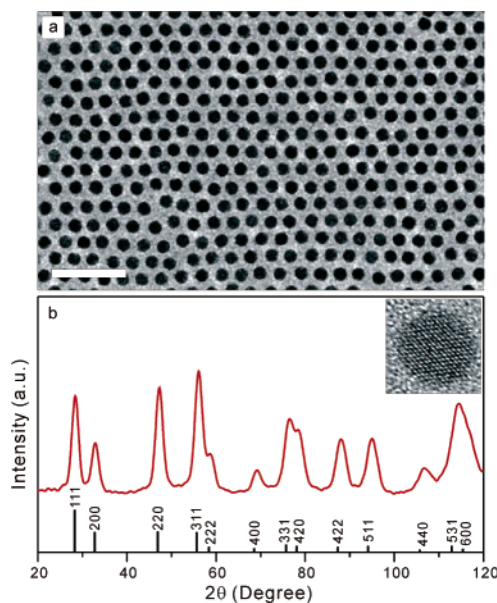


Figure 1. (a) A TEM image of UO₂ nanocrystals made in the typical synthesis. The scale bar is 30 nm. (b) XRD pattern of the UO₂ nanocrystals. The standard diffraction peak positions and relative intensities of bulk cubic UO₂ are indicated. The inset shows a HRTEM image (6.5 nm × 6.5 nm) of the nanocrystal sample.

the synthesis exhibits very stable nanocrystal formation kinetics. Among different syntheses experiments (with the same conditions), the typical deviations of experimental data (in terms of final nanocrystal size and size distribution) are less than 3.0%. Such a highly reproducible synthesis allows a detailed mechanistic analysis of nanocrystal formation by comparing experimental data from different experiments.

To understand the functions of OA and OAm in uranium–dioxide nanocrystal formation, we systematically investigated how the molar ratio between OA and OAm affects the size of final nanocrystals (Figures 2a–c and 3a). A series of synthesis experiments was carried out with nine different OA/OAm ratios, but with the same amount of OA + OAm (4.0 g), ODE (1.0 g), and UAA (0.4 mmol). With the increase of the OA/OAm ratio, the size of the final nanocrystals increased, and a maximum size was obtained when the ratio was 1:1. Then the size of final nanocrystals decreased with a further increase of the molar ratio (Figures 2a–c and 3a). However, the reaction yield was not significantly changed with the increase of the OA/OAm ratio.⁶ Taken together, these results indicate that a minimum number of stable nuclei were formed at the OA/OAm ratio of 1:1, and the increase of either OA or OAm led to an increase of stable nuclei—but a decrease of final nanocrystal size.⁷

Moreover, the size of nanocrystals from the synthesis with OA/OAm ratio of 1:1 is larger than that of the final particles from the original synthesis (6.2 vs 5.4 nm). The difference between these two syntheses is only the total amount of OA + OAm (4.0 vs 2.0 g). This result may indicate that increasing the amount of the OA/OAm mixture at the ratio of 1:1 can lead to larger final nanocrystals.

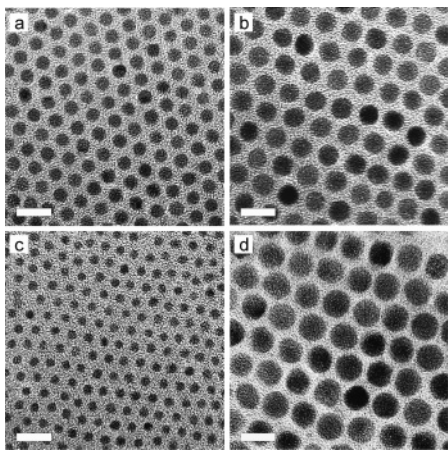


Figure 2. (a–c) TEM image of UO_2 nanocrystals from synthesis with OA/OAm ratios of 1:3, 1:1, and 3:1, respectively. (d) A TEM image of the nanocrystals from a synthesis with UAA (0.4 mmol), ODE (1.0 g), OA (10 g), and OAm (10 g). The scale bar is 10 nm.

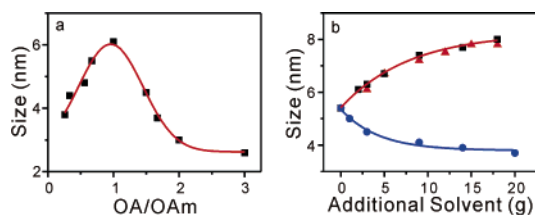


Figure 3. (a) A plot of nanocrystal size in diameter as a function of OA/OAm molar ratio from various syntheses. (b) A plot of nanocrystal size in diameter as a function of the amount of additional solvents added into the original synthesis: black squares for the mixture of OA and OAm at a molar ratio of 1:1, red triangles for OOA, and blue dots for ODE.

To examine the generality of this conclusion, we carried out five further synthesis experiments with various additional amounts of the OA/OAm mixture.⁶ Indeed, the size of the final nanocrystals increased with the increase of the amount of the OA/OAm mixture, and 8-nm particles were produced when the amount is 18 g (Figures 2d and 3b). Thus, a fundamental question is raised on how the amount of the OA/OAm mixture can affect the final nanocrystal size.

IR analyses show that UO_2 nanocrystal formation is accompanied by the formation of *N*-(*cis*-9-octadecenyl)oleamide (OOA) due to the condensation reaction of OA and OAm.⁶ This result suggests that the OA/OAm mixture may affect UO_2 nanocrystal synthesis through the condensation reaction. ¹H NMR analyses further indicated that the condensation reaction can be nearly complete before the nucleation of UO_2 nanocrystals;⁶ therefore, the products of the condensation reaction should play significant roles in controlling the formation of UO_2 nanocrystals.

Two major products of the condensation reaction are water and OOA. To test the effect of water, we carried out UO_2 synthesis while adding water during the experiments.⁶ However, the results show that water does not significantly affect the size of the final products,⁶ thus indicating that OOA should affect the formation of UO_2 nanocrystals.

To examine the detailed effect of OOA, we first synthesized OOA according to a literature method.⁸ Then, six UO_2 synthesis experiments were carried out on the basis of the original synthesis (UAA, 0.4 mmol; OA, 1.0 g; OAm, 1.0 g; and ODE, 1.0 g) but with various amounts of additional pure OOA.⁶ The results from these experiments show that the size of final particles does increase with the amount of additional OOA (Figure 3b). Significantly, the effect of OOA almost perfectly matches that of the mixture of OA/OAm at the molar ratio of 1:1 (the red line in Figure 3b). These

results provide unambiguous evidence that it is OOA—not the mixture of OA and OAm—that plays the major role in controlling the formation of UO_2 nanocrystals.

Furthermore, to identify whether the amide functional group or the hydrocarbon chain on OOA generates the effect on UO_2 nanocrystal formation, we carried out five syntheses based on the conditions used in the original synthesis but with different amounts of additional ODE. The results show that additional ODE leads to an opposite effect on UO_2 nanocrystal formation, a decrease of the size of the final products (Figure 3b). Therefore, the amide functional group on OOA should generate the major effect on the formation of UO_2 nanocrystals.

Interestingly, IR analysis of purified UO_2 nanocrystals shows conclusive evidence that OOA is not on the nanocrystal surface, but the nanocrystals are passivated by OA through chelating bidentate interaction.⁶ Therefore, the effect of OOA on the nanocrystal synthesis is likely achieved through tuning the reactivity of the intermediate states (or active monomers) in the formation of UO_2 particles. Such an effect could lead to a decreased number of stable nuclei and then an increased size of final nanocrystals.

In conclusion, we have developed an organic-phase synthesis method for making high-quality, colloidal UO_2 nanocrystals. These UO_2 nanocrystals are potentially important to applications such as nuclear fuel materials, catalysts, and thermopower materials. Second, we have mapped out the functions of the solvents (OA, OAm, and ODE) in the synthesis, and we found that OOA—a product of the condensation of OA and OAm—can substantially affect the formation of UO_2 nanocrystals. Importantly, these results provide fundamental insight into the mechanisms of UO_2 nanocrystal synthesis. In addition, because a mixture of OA and OAm has been widely used in synthesizing a variety of high-quality metal or metal-oxide nanocrystals,^{9–12} the results herein should also be important for understanding the detailed mechanisms of these syntheses.

Acknowledgment. This work was supported by the University of Florida, ACS Petroleum Research Fund, and the Office of Naval Research.

Supporting Information Available: Detailed synthetic procedure, IR, NMR, XRD, and TEM images. This material is available free of charge via the Internet at <http://pubs.acs.org>.

References

- (1) (a) Bodansky, D. *Nuclear Energy: Principles, Practices, and Prospects*, 2nd ed.; Springer: New York, 2004. (b) Forsberg, C. W. *Nucl. Technol.* **2000**, *131*, 337.
- (2) (a) Hutchings, G. J.; Heneghan, C. S.; Hudson, I. D.; Taylor, S. H. *Nature* **1996**, *384*, 341. (b) Zhang, Z. T.; Konduru, M.; Dai, S.; Overbury, S. H. *Chem. Commun.* **2002**, 2406.
- (3) Ruello, P.; Petot-Ervas, G.; Petot, C.; Desgranges, L. *J. Am. Ceram. Soc.* **2005**, *88*, 604.
- (4) (a) Kan, S.; Mokari, T.; Rothenberg, E.; Banin, U. *Nat. Mater.* **2003**, *2*, 155. (b) Xia, Y.; Yang, P.; Sun, Y.; Wu, Y.; Mayers, B.; Gates, B.; Yin, Y.; Kim, F.; Yan, H. *Adv. Mater.* **2003**, *15*, 353. (c) Alivisatos, A. P. *Nat. Biotechnol.* **2004**, *22*, 47. (d) Zhu, L.; Zhu, M.-Q.; Hurst, J. K.; Li, A. D. Q. *J. Am. Chem. Soc.* **2005**, *127*, 8968. (e) Fan, H. Y.; Gabaldon, J.; Brinker, C. J.; Jiang, Y. B. *Chem. Commun.* **2006**, 2323.
- (5) O'Loughlin, E. J.; Kelly, S. D.; Cook, R. E.; Csencsits, R.; Kemner, K. M. *Environ. Sci. Technol.* **2003**, *37*, 721.
- (6) See Supporting Information.
- (7) Cao, Y. C.; Wang, J. *J. Am. Chem. Soc.* **2004**, *126*, 14336.
- (8) Zubarev, E. R.; Pralle, M. U.; Sone, E. D.; Stupp, S. I. *J. Am. Chem. Soc.* **2001**, *123*, 4105.
- (9) Zhang, Z. H.; Zhong, X. H.; Liu, S. H.; Li, D. F.; Han, M. Y. *Angew. Chem., Int. Ed.* **2005**, *44*, 3466.
- (10) (a) Chen, M.; Kim, J.; Liu, J. P.; Fan, H.; Sun, S. *J. Am. Chem. Soc.* **2006**, *128*, 7132. (b) Sun, S.; Zeng, H.; Robinson, D. B.; Raoux, S.; Rice, P. M.; Wang, S. X.; Li, G. *J. Am. Chem. Soc.* **2004**, *126*, 273.
- (11) Mai, H.-X.; Zhang, Y.-W.; Si, R.; Yan, Z.-G.; Sun, L.-D.; You, L.-P.; Yan, C.-H. *J. Am. Chem. Soc.* **2006**, *128*, 6426.
- (12) (a) Liu, Q.; Lu, W.; Ma, A.; Tang, J.; Lin, J.; Fang, J. *J. Am. Chem. Soc.* **2005**, *127*, 5276. (b) Stowell, C. A.; Korgel, B. A. *Nano Lett.* **2005**, *5*, 1203. (c) Lee, D. C.; Ghezelbash, A.; Stowell, C. A.; Korgel, B. A. *J. Phys. Chem. B* **2006**, *110*, 20906.

JA067940P